

Electrodynamics of BaFe₂As₂ from infrared measurements under pressureL. Baldassarre,¹ A. Perucchi,¹ P. Postorino,² S. Lupi,^{1,2} C. Marini,^{2,3} L. Malavasi,⁴ J. Jiang,⁵ J. D. Weiss,⁵
E. E. Hellstrom,⁵ I. Pallecchi,⁶ and P. Dore⁷¹*Sincrotrone Trieste, Area Science Park, 34012 Trieste, Italy*²*CNR-IOM and Dipartimento di Fisica, Università di Roma "Sapienza," Piazzale Aldo Moro 2, 00185 Rome, Italy*³*European Synchrotron Radiation Facility, BP 220, 38043 Grenoble Cedex, France*⁴*Dipartimento di Chimica Fisica M. Rolla, INSTM (UdR Pavia) and IENI-CNR, Università di Pavia, Viale Taramelli 16, 27100 Pavia, Italy*⁵*Applied Superconductivity Center, National High Magnetic Field Laboratory, Florida State University,**2031 East Paul Dirac Drive, Tallahassee, Florida 32310, USA*⁶*CNR-SPIN, Corso Perrone 24, 16152 Genova, Italy*⁷*CNR-SPIN and Dipartimento di Fisica, Università di Roma "Sapienza," Piazzale Aldo Moro 2, 00185 Rome, Italy*

(Received 20 January 2012; revised manuscript received 18 April 2012; published 23 May 2012)

We report on an infrared study on the undoped compound BaFe₂As₂ as a function of pressure (up to about 10 GPa) at three temperatures (300, 160, and 110 K). The evolution with pressure and temperature of the optical conductivity shows that by increasing pressure, the mid-infrared absorptions associated with magnetic order are lowered while the Drude term increases, indicating the evolution towards a conventional metallic state. We evaluate the spectral weight dependence on pressure comparing it to that previously found upon doping. All the optical results indicate that lattice modifications cannot be recognized as the only parameter determining the low-energy electrodynamic in these compounds.

DOI: [10.1103/PhysRevB.85.174522](https://doi.org/10.1103/PhysRevB.85.174522)

PACS number(s): 74.25.Gz, 62.50.-p, 78.30.-j

I. INTRODUCTION

The discovery of superconductivity in pnictides¹ has triggered tremendous interest in a large scientific community. Despite the large experimental and theoretical efforts,^{2,3} many questions are left unanswered, in particular concerning the subtle interplay among electronic, magnetic, and structural degrees of freedom.

The common characteristic of these systems is that the undoped parent compounds have a metallic behavior, and undergo a transition from a high-temperature paramagnetic phase to an antiferromagnetic spin-density-wave (SDW) state at the temperature T_{SDW} (~ 150 K), accompanied by a tetragonal to orthorhombic (or monoclinic) structural transition. Upon entering the SDW state, the Fermi surface of these multiband systems is only partially gapped; therefore the metallic state persists in spite of the reduction of the carrier density. Superconductivity is achieved, below T_c , either by electron (or hole) doping or, in the undoped parent compounds, by applying external pressure.⁴ Furthermore, in the case of superconducting systems, the applied pressure can remarkably enhance T_c .⁵ It is now known that structure and properties of chemically doped samples are strongly linked;^{6,7} for example a decrease of the Fe-Fe distance (that occurs upon chemical doping) has been found to strongly enhance T_c . A similar lattice modification was found also in the case of applied pressure⁸ and the idea has been put forward that the structural changes play a major role in determining the electrodynamic properties. It is thus clear that a complex interplay among different degrees of freedom is at work in these systems,⁹ which makes challenging the understanding of their intriguing physical properties.

The complex phase diagram of pnictides has been carefully addressed in particular in systems of the so-called 122 family AFe₂As₂ ($A = \text{Ba, Sr, Ca, Eu}$): Superconductivity is here obtained either by chemical substitutions in the A plane

(hole doping) or in the Fe-As layer (electron doping), and large effects have been reported as a function of physical pressure.^{5,8,10} For the undoped compounds, in particular, it has been shown that pressure progressively lowers T_{SDW} , eventually suppressing the structural/magnetic transition, and can originate the insurgence of the superconducting phase at the cost of the SDW state. The same effect can be achieved by means of a chemical pressure by replacing smaller P atoms for the larger As atoms, with no effect of charge doping.¹¹ Most authors agree on the fact that chemical and physical pressure act similarly on these compounds; however it was recently pointed out that in Co-doped compounds the evolution of the Fe-As distance is different¹² with physical and chemical pressure (by replacing As with P). As this parameter is considered to be crucial in determining the properties of pnictides, a deeper insight into the equivalence doping-pressure is thus required.

Several infrared studies have been performed on iron-based superconductors to probe both the normal and the superconducting state.^{13–16} In 122 systems, in particular, studies have been performed in order to assess the effect of the magnetic transition at T_{SDW} on the electronic structure. A general consensus has been achieved on the existence in the ab -plane optical response of at least two electronic subsystems, which can be described by two Drude contributions in the frequency-dependent conductivity. In these two contributions, characterized by different scattering rates, the transition to the low-temperature SDW state can be the origin of the opening of energy gaps with transfer of optical spectral weight from low to high frequencies.^{16,17}

Recently particular attention has been devoted to the study of the degree of electronic correlations,^{18–20} that is, the ratio between the experimental kinetic energy (K_{exp}) and that obtained through band calculations (K_{theory}) often performed in the local density approximation. A value K_{exp}/K_{theory} close to 1 indicates a *conventional* metallic state (i.e., with no

tendency towards charge localization due to correlations) while the opposite limit $K_{\text{exp}}/K_{\text{theory}} \rightarrow 0$ identifies a system with fully localized electrons. Although this interpretation of the $K_{\text{exp}}/K_{\text{theory}}$ parameter has to be taken with some caution,^{20,21} especially in multiband systems, it has been shown that¹⁸ there is a similar tendency towards localization^{18,20} in different families of high T_c and that this parameter might be a key ingredient in high- T_c superconductivity.^{18,20} In the above sketched scenario, infrared measurements are of basic interest since the integral of the Drude contribution to the frequency-dependent conductivity (i.e., the Drude spectral weight) simply mimics the kinetic energy of the free carriers. Moreover, an infrared study performed as a function of temperature and pressure on undoped pnictides, avoiding disorder or local distortions induced by doping, yields information on the pressure-driven changes in the frequency-dependent conductivity, i.e., in the charge dynamics.

In the present work, we report on an infrared investigation on the undoped compound BaFe_2As_2 as a function of pressure at three temperatures, 110 K, 160 K, and 300 K, i.e., above and below T_{SDW} at ambient condition. By evaluating the evolution of the infrared spectral weight with pressure, and comparing it to that found upon doping, we find that lattice modifications cannot be recognized as the only parameter determining the low-energy electrostatics in these compounds.

II. EXPERIMENTAL DETAILS

Infrared reflectance measurements were performed on high-quality BaFe_2As_2 single crystals ($T_{\text{SDW}} = 140$ K at ambient pressure). The crystals were prepared by the self-flux method.²² Ba pieces, Fe powder, and As particles were mixed together according to the ratio of Ba:Fe:As = 1:4:4. After mixing, the powder was wrapped with Nb foil and placed in a stainless steel ampoule. The ampoule was evacuated, welded shut, and compressed with a cold isostatic press at 275 MPa to press the powder into a pellet. The heat treatment was done in a hot isostatic press at 193 MPa. The samples were held for 9 hours at 1120 °C, and ramped down to 910 °C at 2 °C/h and then cooled to room temperature in a hour. The pressure was released at the end of the heat treatment. The single crystals were extracted by breaking the reacted pellet. Data were collected on increasing pressure P up to a value of 10 GPa, at different temperatures T between room T and 110 K.

Pressure-dependent reflectivity measurements were performed with a diamond anvil cell (DAC). A 50 μm thick CuBe gasket was placed in a screw-driven opposing-plate DAC, equipped with type IIa diamonds. A small piece of the sample had been cut and placed over a pre-sintered CsI pellet in the hole drilled in the gasket. The good quality of surface obtained by breaking the sample allowed having a clean sample-diamond (s-d) interface. The DAC was mounted inside a N_2 -flow microscope cryostat from Oxford, allowing us to cool the DAC down to ≈ 100 K. In order to determine both pressure and temperature of the sample, a ruby chip was placed inside the sample chamber while a second one was placed on the external face of the diamond. The pressure value was measured *in situ* by the standard ruby fluorescence²³ technique. Since the shift of the two fluorescence lines depends strongly

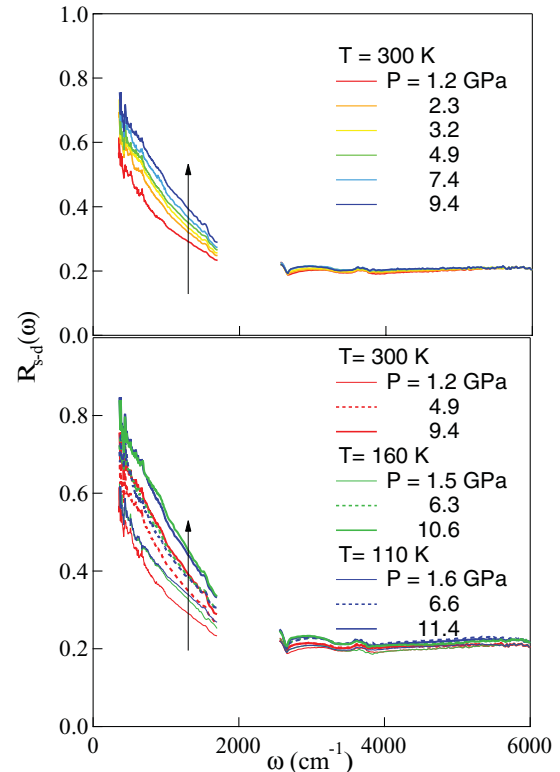


FIG. 1. (Color online) Upper panel: Room temperature reflectivity at the sample-diamond interface shown in the 0–6000 cm^{-1} frequency range for different pressures (indicated in figure). Lower panel: Reflectivity at the sample-diamond interface along three pressure-temperature cycles. Upon cooling down the pressure value increases significantly and sets back to the starting value once room temperature is reached again. The arrows indicate the direction of increasing pressure.

on both T and P , measurements were performed separately on the two ruby chips: on the external one to determine T and on the internal for P . We remark that by measuring the T -induced shift of the ruby line, we determine precisely the temperature of the sample which is in tight contact with the highly conducting diamond anvil. The spacing, the linewidth, and the deep hole between the two ruby fluorescence lines are rather delicate markers of the hydrostaticity of the sample environment. Those have been monitored up to the highest measured pressure, ensuring us of being in reasonably good hydrostatic conditions.

The incident and reflected light were focused and collected with an optical microscope mounting Cassegrain objectives and equipped with a mercury-cadmium-telluride (MCT) detector and a bolometer. The microscope was coupled to the IFs66/v Bruker Michelson interferometer. This measuring configuration allowed us to explore the 300–12000 cm^{-1} spectral range.²⁴ Due to the small size of the sample, the high brilliance of synchrotron radiation at the SISSI beamline at the ELETTRA storage ring²⁵ was exploited, with a great advantage especially for the measurements in the spectral region of the far-infrared. The measurement procedure was the same as described in Refs. 26 and 27.

III. RESULTS AND DISCUSSION

The reflectivity at the sample-diamond interface (R_{s-d}) is shown in Fig. 1 in the 0–6000 cm^{-1} frequency range for various pressures and temperatures. Data are not shown in the 1600–2700 cm^{-1} range due to the strong phonon absorption of the diamonds.²⁸ All curves merge at about 6000 cm^{-1} , showing no pressure or temperature dependence above such frequency. At room temperature, all curves increase for decreasing frequency suggesting a metallic-like behavior and, by applying pressure, the reflectivity is enhanced in the whole energy range pointing to an increased metallic behavior. As $T < T_{\text{SDW}}$ ($P = 1.6$ GPa, $T = 110$ K) R_{s-d} increases its value in the mid-IR but shows only a small increase at low frequency almost crossing the reflectivity curve recorded for $P = 1.2$ GPa and $T = 300$ K.

To obtain the optical conductivity $\sigma_1(\omega)$ (real part of the complex conductivity) we have fitted the reflectivity with a Drude-Lorenz model, taking into account the sample-diamond interface.²⁹ This has been done by first modeling the refractive index $\tilde{n} = n + ik$ as follows:³⁰

$$\epsilon_1 = n^2 - k^2 = \epsilon_\infty + \sum_i \frac{S_i^2(\omega_i^2 - \omega^2)}{(\omega_i^2 - \omega^2)^2 + \Gamma_i^2\omega^2}, \quad (1)$$

$$\epsilon_2 = 2nk = \sum_i \frac{S_i^2\Gamma_i\omega}{(\omega_i^2 - \omega^2)^2 + \Gamma_i^2\omega^2}, \quad (2)$$

where S_i , Γ_i , and ω_i are respectively the oscillator strength, its width, and its central frequency. The Drude contribution

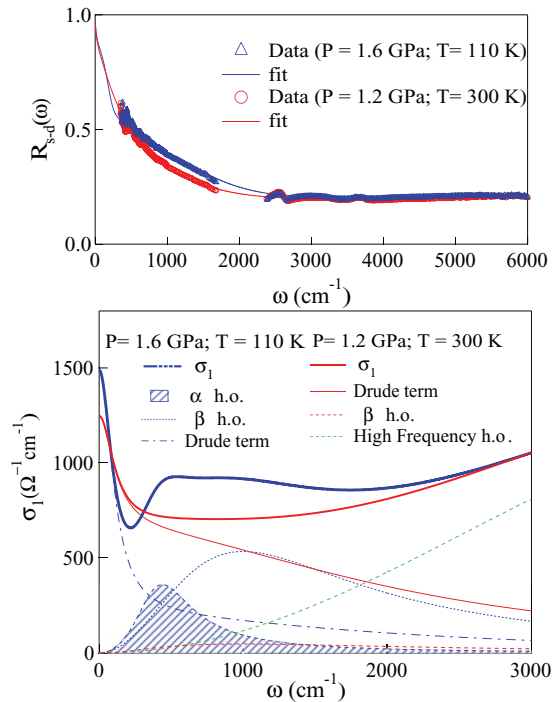


FIG. 2. (Color online) Upper panel: Reflectivity at the sample diamond interface compared with the best Drude-Lorenz fit. Lower panel: Optical conductivity $\sigma_1(\omega)$ obtained from the fitting procedure for $T = 110$ K and 300 K. The fit components are also reported: the sum of the two Drude terms and the harmonic oscillators (h.o.). The high-frequency oscillator (which mimics the contributions above the measured frequencies) is kept constant for all the measured curves.

is obtained once $\omega_i = 0$. The reflectivity is thus modeled by using

$$R_{s-d} = \left| \frac{\tilde{n} - \tilde{n}_D}{\tilde{n} + \tilde{n}_D} \right|^2, \quad (3)$$

where \tilde{n}_D is the refractive index of diamond from Ref. 28.

We considered two Drude terms and three harmonic oscillators (h.o.), as proposed by S. J. Moon and coworkers³¹ and successfully used by other authors.^{32,33} A high-frequency h.o. has been used to mimic the absorptions that take place above the highest measured frequency and has been kept constant for all curves. Two Drude terms, one narrow and one broad, are necessary to fit our data. It is noteworthy that this decomposition of the spectra holds for all the compounds of the 122 family.^{31,33,34} The lack of low-frequency data prevents in our case an unambiguous determination of the spectral weight (SW) of each Drude component, while the SW of their sum ends up being well determined.

Two oscillators (which we call α and β , similarly to the notation in Ref. 31) are needed to achieve satisfactory fittings in the mid-IR region below the SDW transition, while only one (β) is enough for $T > T_{\text{SDW}}$. In Fig. 2 we show the fitting curves together with the experimental data for 300 and 110 K and 1.2 and 1.6 GPa, i.e., in the normal and in the SDW state, respectively. For both the states, the resulting optical conductivity and the corresponding components are shown in the lower panel of Fig. 2: As the SDW state sets in, there is a depletion of the conductivity below 500 cm^{-1} and the formation of strong mid-IR absorption bands above this frequency. At much lower frequencies the onset of the narrow Drude component is visible. The SDW transition therefore results in a spectral weight transfer from the Drude terms to the α and β oscillators.

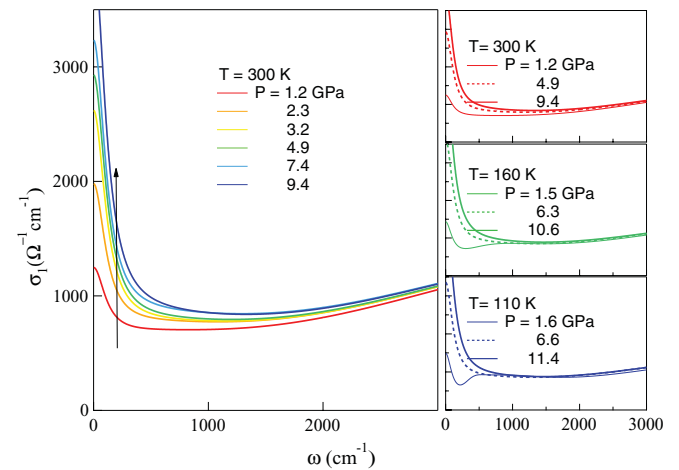


FIG. 3. (Color online) Left: Optical conductivity $\sigma_1(\omega)$ at various pressures at room temperature. The arrow indicates the direction of increasing pressure. As pressure is increased the conductivity increases in the whole shown range. Right: $\sigma_1(\omega)$ at 300, 160, and 110 K. At the lowest measured pressure (1.6 GPa), as the SDW state sets in, $\sigma_1(\omega)$ shows a depletion and a peak respectively below and slightly above 500 cm^{-1} due to the partial gapping of the Fermi surface. At lower frequency it is possible to see the onset of a narrow Drude component.

The optical conductivity $\sigma_1(\omega)$ is plotted in Fig. 3 at selected temperatures and pressures. At room temperature the conductivity increases its absolute value with increasing pressure, especially towards low frequency, indicating that the system tends towards a more metallic state. This is clearly evident from the pressure evolution of the Drude SW, shown in the upper panel of Fig. 4. On the other hand, as pressure is increased, the SW of the absorption band in the mid-IR at room temperature remains almost constant and then decreases above 9 GPa. The SW of the β h.o. decreases with increasing P also at 110 and 160 K as expected due to the progressive suppression of the magnetic state with pressure ($dT_{SDW}/dP < 0$), as reported by several authors.^{5,35,36} The SW of the β oscillator in the mid-IR at 160 K and 110 K, for $P > 6$ GPa, is comparable with the SW attained at room temperature, suggesting that above this pressure the system is not undergoing any appreciable electronic phase transition. Once the SDW transition is suppressed, the external parameter that mainly drives the optical response is pressure, with only a small effect due to temperature. Note that by applying pressure, the overall SW increases and it is not recovered in the measured spectral range.

An accurate determination of the optical conductivity $\sigma_1(\omega)$ allows us to follow the evolution upon external parameters

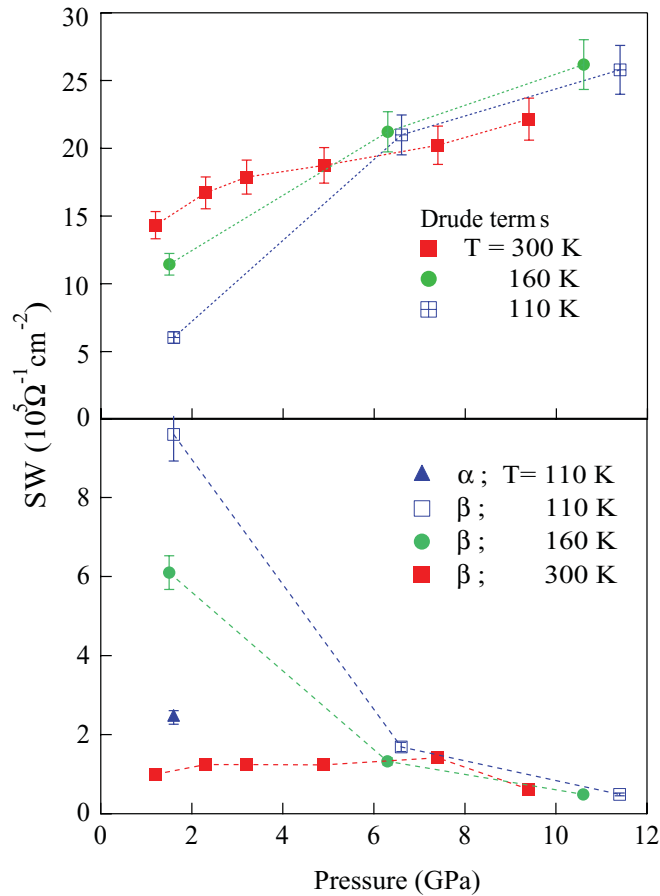


FIG. 4. (Color online) Pressure-dependent changes in the spectral weight (SW) at 110 K (blue), 160 K (green), and 300 K (red) for the Drude terms (upper panel) and the mid-IR harmonic oscillator (lower panel). The lines are only a guide for the eye.

of both free carrier response (Drude terms) and interband excitations (harmonic oscillators centered at finite frequency). The outcome of the fitting procedure determines also the integral of the Drude contribution to $\sigma_1(\omega)$, i.e., the Drude spectral weight. In order to evaluate the degree of correlation previously introduced, we considered the ratio between the experimental kinetic energy ($K_{D-\text{exp}}$) directly provided by the Drude spectral weight (see Ref. 19 for the complete formula), and the theoretical kinetic energy (K_{theory}) given¹⁹ by the square of the plasma frequency ω_p , obtained as a function of pressure in the paramagnetic phase by means of density functional theory (DFT) computations³⁷ (see Fig. 5). Despite the light increase of ω_p with pressures up to 10 GPa, the resulting $K_{D-\text{exp}}/K_{\text{theory}}$ ratio increases smoothly on increasing pressure indicating that the system is shifting towards a conventional metallic state. It is worth noticing that the value that we find at the lowest measured pressure (~ 0.2) is in good agreement with what is found (0.25–0.29) at ambient conditions by other authors.^{18,20} A comparison between pressure and doping dependence of the degree of correlation is impossible, since its value was only reported for $\text{BaFe}_{1.84}\text{Co}_{0.16}\text{As}_2$ and its evolution with doping is not reported in the literature.

A different, fully experimental approach to evaluate the degree of correlation has been proposed by Degiorgi and coworkers:^{33,38} Instead of comparing the experimental kinetic energy with a theoretical value, they discuss the ratio between the experimental kinetic energy given by the Drude spectral weight and the SW of $\sigma_1(\omega)$ including both Drude and mid-IR contributions (K_{band}). They find a degree of correlation $K_{D-\text{exp}}/K_{\text{band}}$ lower than 0.65 for the superconducting samples $[\text{Ba}(\text{Co}_x\text{Fe}_{1-x})_2\text{As}_2$ with $x < 0.11$] and higher (~ 0.7) as the system becomes overdoped. In order to compare the effect of pressure and Co doping on the degree of correlation we have also calculated the ratio $K_{D-\text{exp}}/K_{\text{band}}$. For this comparison we used the scaling relation proposed by Drotzinger

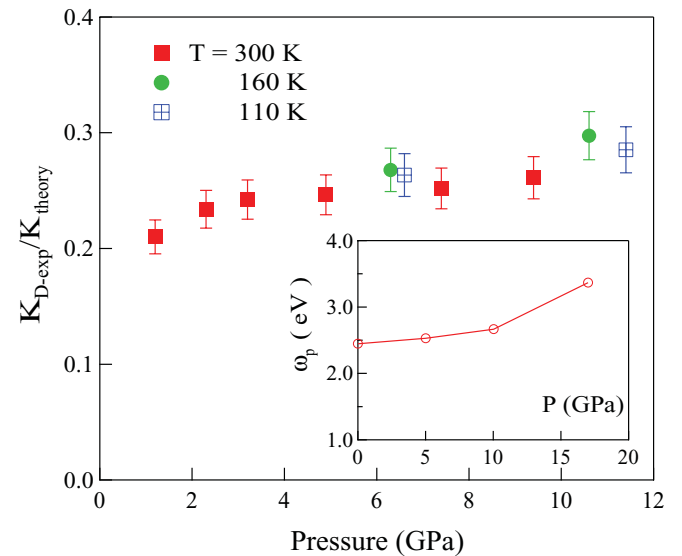


FIG. 5. (Color online) $K_{D-\text{exp}}/K_{\text{theory}}$ plotted for increasing pressure in the paramagnetic phase. Plasma frequency values obtained by DFT calculations (Ref. 37) are reported in the inset.

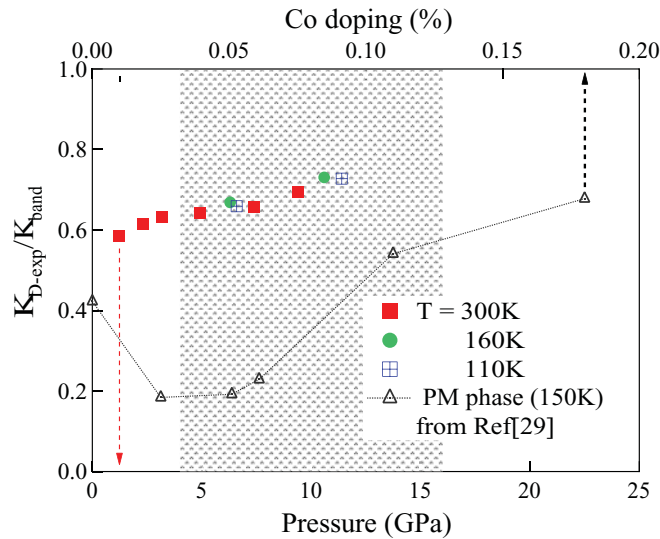


FIG. 6. (Color online) $K_{D\text{-exp}}/K_{\text{band}}$ plotted for increasing pressure at 110, 160, and 300 K (all in the paramagnetic phase) compared with data from Ref. 33. The gray shaded area identifies the regions (upon Co doping and pressure) where superconductivity is attained.

et al.:³⁹ By means of transport and magnetic measurements in the superconducting region, they suggested $\Delta P/\Delta x \approx 1.275$ GPa/%Co. In Fig. 6 we plot the $K_{D\text{-exp}}/K_{\text{band}}$ ratio for our data in the paramagnetic phase together with data (also in the paramagnetic phase) on Co-doped compounds (from Ref. 33). We remark that we are not putting the accent on the differences of the absolute value of this parameter (which could depend also on details of the high-frequency extrapolation when performing KK analysis) but rather on its different evolution with doping and pressure. Suppose starting at the same value for undoped compound at ambient conditions; for low doping/pressure, chemical doping and pressure act differently: The former yields $K_{D\text{-exp}}/K_{\text{band}}$ values lower than those given by pressure, at odds with the fact that inserting Co in the FeAs planes not only modifies the lattice parameters but also injects one carrier per dopant ion. It was shown that both pressure and doping suppress the magnetic/structural transitions but only certain dopants (i.e., certain doping levels) allow superconducting pairing.⁴⁰ We know that upon doping BaFe₂As₂ with Co, for $x < 0.12$, the SW of the mid-IR absorption bands is strongly increased, at odds with the SW of the Drude term,³³ suggesting that spin fluctuations are enhanced while long-range magnetic order is suppressed. This probably is one of the key factors in originating superconductivity once the structure is modified *enough* due to the random insertion of Co ions. On the other hand, by applying pressure, the magnetic/structural transition is suppressed but the SW of the mid-IR contributions is

reduced, suggesting that the magnetic fluctuations are lowered, probably due to reduced anisotropy and weaker nesting.⁴¹ The reduction of lattice parameters is enough for quenching the SDW state (and, at lower temperatures, to originate superconductivity), even though the system tends towards a fairly conventional metallic state. For $x > 0.12$ the slope of $K_{D\text{-exp}}/K_{\text{band}}$ values for Co-doped samples becomes similar to what we have measured under pressure, suggesting that once the system is in the overdoped regime, a common mechanism is driving the suppression of superconductivity.

In conclusion, we have studied the infrared response of BaFe₂As₂ under pressure down to 110 K. We remark that pressure-dependent IR measurements can give the unique opportunity to go beyond the zero-frequency conductivity, providing information on the low energy charge dynamics. We observe no signature in the optical conductivity of SDW ordering in this temperature range when $P \geq 3$ GPa, in agreement with the results of previous transport measurements. It has been possible to follow the evolution with pressure of the spectral weight of both Drude and mid-IR contributions, showing that the system tends towards a conventional metallic state and that the absorptions associated with fluctuative magnetic order are lowered by increasing pressure. On the basis of the obtained results we could compare the effect of pressure and Co doping on the degree of correlation. The obtained results reported in Fig. 6 indicate that in the underdoped regime, pressure and Co doping favor the onset of superconductivity (destroy long-range magnetic order) by following different mechanisms displaying opposite effects on the degree of correlation parameter. On the other hand, at high pressure/doping the correlation degree monotonically increases in both cases, thus suggesting that an increased itinerancy is the common mechanism for T_c reduction in the overdoped regime. Our results indicate that the lattice distortions cannot alone explain the evolution of the electrodynamics of underdoped compounds compared to that of the undoped sample under pressure since the routes taken to suppress the SDW and favor superconductivity are different in the two cases. A more realistic description of the interplay between different degrees of freedom is needed to understand the physics of pnictides.

ACKNOWLEDGMENTS

We wish to thank M. Putti for providing the samples, and G. Profeta and A. Continenza for useful discussions and for providing ω_p values computed at a number of pressures prior to publication. We acknowledge financial support from PRIN Project No. 2008XWLVF9-002 and from the CARIPLIO Foundation (Project No. 2009-2540). The work at FSU was supported by NSF DMR-1006584 and 0084173, and by the State of Florida.

¹Y. Kamihara, T. Watanabe, M. Hirano, and H. Hosono, *J. Am. Chem. Soc.* **130**, 3296 (2008).

²K. Ishida, Y. Nakai, and H. Hosono, *J. Phys. Soc. Jpn.* **78**, 062001 (2009).

³G. R. Stewart, *Rev. Mod. Phys.* **83**, 1589 (2011).

⁴C. W. Chu and B. Lorenz, *Physica C* **469**, 385 (2009).

⁵K. Ahilan, F. L. Ning, T. Imai, A. S. Sefat, M. A. McGuire, B. C. Sales, and D. Mandrus, *Phys. Rev. B* **79**, 214520 (2009).

- ⁶M. Rotter, M. Pangerl, M. Tegel, and D. Johrendt, *Angew. Chem., Int. Ed.* **47**, 7949 (2008).
- ⁷J. Zhao, Q. Huang, C. de la Cruz, S. Li, J. W. Lynn, Y. Chen, M. A. Green, G. F. Chen, G. Li, Z. Li, J. L. Luo, N. L. Wang, and P. Dai, *Nature Mater.* **7**, 953 (2008).
- ⁸S. A. J. Kimber, A. Kreyssig, Y. Z. Zhang, H. O. Jeschke, R. Valenti, F. Yokaichiya, E. Colombier, J. Yan, T. C. Hansen, T. Chatterji, R. J. McQueeney, P. C. Canfield, A. I. Goldman, and D. N. Argyriou, *Nature Mater.* **8**, 471 (2009).
- ⁹Z. P. Yin, K. Haule, and G. Kotliar, *Nature Mater.* **10**, 932, (2011).
- ¹⁰W. J. Duncan, O. P. Welzel, C. Harrison, X. F. Wang, X. H. Chen, F. M. Grosche, and P. G. Niklowitzet, *J. Phys.: Condens. Matter* **22**, 052201 (2010).
- ¹¹S. Jiang, H. Xing, G. F. Xuan, C. Wang, Z. Ren, C. M. Feng, J. H. Dai, Z. A. Xu, and G. H. Cao, *J. Phys.: Condens. Matter* **21**, 012208 (2009).
- ¹²V. Zinth and D. Johrendt, arXiv:1203.1459.
- ¹³M. Tropeano, C. Fanciulli, C. Ferdeghini, D. Marre, A. S. Siri, M. Putti, A. Martinei, M. Ferretti, A. Palenzona, M. R. Cimberle, C. Mirri, S. Lupi, R. Sopracase, P. Calvani, and A. Perucchi, *Supercond. Sci. Technol.* **22**, 034004 (2009).
- ¹⁴B. Gorshunov, D. Wu, A. A. Voronkov, P. Kallina, K. Iida, S. Haindl, F. Kurth, L. Schultz, B. Holzapfel, and M. Dressel, *Phys. Rev. B* **81**, 060509(R) (2010).
- ¹⁵A. Perucchi, L. Baldassarre, C. Marini, S. Lupi, J. Jiang, J. D. Weiss, E. E. Hellstrom, S. Lee, C. W. Bark, C. B. Eom, M. Putti, I. Pallecchi, and P. Dore, *Eur. Phys. J. B* **77**, 25 (2010).
- ¹⁶D. Wu, N. Barisic, P. Kallina, A. Faridian, B. Gorshunov, N. Drichko, L. J. Li, X. Lin, G. H. Cao, Z. A. Xu, N. L. Wang, and M. Dressel, *Phys. Rev. B* **81**, 100512 (2010).
- ¹⁷Z. G. Chen, T. Dong, R. H. Ruan, B. F. Hu, B. Cheng, W. Z. Hu, P. Zheng, Z. Fang, X. Dai, and N. L. Wang, *Phys. Rev. Lett.* **105**, 097003 (2010).
- ¹⁸D. N. Basov and A. V. Chubukov, *Nature Phys.* **7**, 272 (2011).
- ¹⁹M. M. Qazilbash, J. J. Hamlin, R. E. Baumbach, Lijun Zhang, D. J. Singh, M. B. Maple, and D. N. Basov, *Nature Phys.* **5**, 647 (2009).
- ²⁰A. A. Schafgans, S. J. Moon, B. C. Pursley, A. D. LaForge, M. M. Qazilbash, A. S. Sefat, D. Mandrus, K. Haule, G. Kotliar, and D. N. Basov, *Phys. Rev. Lett.* **108**, 147002 (2012).
- ²¹I. I. Mazin, arXiv:0910.4117v1.
- ²²A. S. Sefat, R. Jin, M. A. McGuire, B. C. Sales, D. J. Singh, and D. Mandrus, *Phys. Rev. Lett.* **101**, 117004 (2008).
- ²³H. K. Mao, P. M. Bell, J. W. Shaner, and D. J. Steinberg, *J. Appl. Phys.* **49**, 3276 (1978).
- ²⁴L. Baldassarre, A. Perucchi, P. Postorino, and S. Lupi, *High Press. Res.* **29**, 639 (2009).
- ²⁵S. Lupi, A. Nucara, A. Perucchi, P. Calvani, M. Ortolani, L. Quaroni, and M. Kiskinova, *J. Opt. Soc. Am. B* **24**, 959 (2007).
- ²⁶L. Baldassarre, A. Perucchi, E. Arcangeletti, D. Nicoletti, D. Di Castro, P. Postorino, V. A. Sidorov, and S. Lupi, *Phys. Rev. B* **75**, 245108 (2007).
- ²⁷M. Lavagnini, A. Sacchetti, L. Degiorgi, E. Arcangeletti, L. Baldassarre, P. Postorino, S. Lupi, A. Perucchi, K. Y. Shin, and I. R. Fisher, *Phys. Rev. B* **77**, 165132 (2008).
- ²⁸P. Dore, A. Nucara, D. Cannavó, G. De Marzi, P. Calvani, A. Marcelli, R. S. Sussmann, A. J. Whitehead, C. N. Dodge, A. J. Krehan and H. J. Peters, *Appl. Opt.* **37**, 5731 (1998).
- ²⁹J. S. Plaskett and P. N. Schatz, *J. Chem. Phys.* **38**, 612 (1963).
- ³⁰G. Burns, *Solid State Physics* (Academic Press, Boston, 1990).
- ³¹S. J. Moon, J. H. Shin, D. Parker, W. S. Choi, I. I. Mazin, Y. S. Lee, J. Y. Kim, N. H. Sung, B. K. Cho, S. H. Khim, J. S. Kim, K. H. Kim, and T. W. Noh, *Phys. Rev. B* **81**, 205114 (2010).
- ³²W. Z. Hu, J. Dong, G. Li, Z. Li, P. Zheng, G. F. Chen, J. L. Luo, and N. L. Wang, *Phys. Rev. Lett.* **101**, 257005 (2008).
- ³³A. Lucarelli, A. Dusza, F. Pfuner, P. Lerch, J. G. Analytis, J.-H. Chu, I. R. Fisher, and L. Degiorgi, *New J. Phys.* **12**, 073036 (2010).
- ³⁴N. Barisic, D. Wu, M. Dressel, L. J. Li, G. H. Cao, and Z. A. Xu, *Phys. Rev. B* **82**, 054518 (2010).
- ³⁵A. Mani, N. Ghosh, S. Paulraj, A. Bharathi, and C. S. Sundar, *Europhys. Lett.* **87**, 17004 (2009).
- ³⁶F. Ishikawa, N. Eguchi, M. Kodama, K. Fujimaki, M. Einaga, A. Ohmura, A. Nakayama, A. Mitsuda, and Y. Yamada, *Phys. Rev. B* **79**, 172506 (2009).
- ³⁷G. Profeta (unpublished).
- ³⁸L. Degiorgi, *New J. Phys.* **13**, 023011 (2011).
- ³⁹S. Drotzinger, P. Schweiss, K. Grube, T. Wolf, P. Adelman, C. Meingast, and H. v. Löhneysen, *J. Phys. Soc. Jpn.* **79**, 124705 (2010).
- ⁴⁰N. Ni, A. Thaler, J. Q. Yan, A. Kracher, E. Colombier, S. L. Budko, P. C. Canfield, and S. T. Hannahs, *Phys. Rev. B* **82**, 024519 (2010).
- ⁴¹A. Sacchetti, E. Arcangeletti, A. Perucchi, L. Baldassarre, P. Postorino, S. Lupi, N. Ru, I. R. Fisher, and L. Degiorgi, *Phys. Rev. Lett.* **98**, 026401 (2007).